

- ¹W. T. Anderson, F. C. Thatcher, and R. R. Hewitt, *Phys. Rev.* **171**, 541 (1968).
- ²F. C. Thatcher and R. R. Hewitt, *Phys. Rev. B* **1**, 454 (1970).
- ³A. Blandin and E. Daniel, *J. Phys. Chem. Solids* **10**, 126 (1959).
- ⁴T. J. Rowland, *Phys. Rev.* **125**, 459 (1962).
- ⁵R. E. Watson, L. H. Bennett, and A. J. Freeman, *Phys. Rev.* **179**, 590 (1969).
- ⁶E. P. Jones and D. L. Williams, *Can. J. Phys.* **42**, 1499 (1964).
- ⁷F. Borsa and R. G. Barnes, *J. Phys. Chem. Solids* **25**, 1305 (1964).
- ⁸S. N. Sharma, thesis (University of British Columbia, 1967) (unpublished).
- ⁹J. F. Adams, B. F. Williams, and R. R. Hewitt, *Phys. Rev.* **151**, 238 (1966).
- ¹⁰A. C. Chapman, P. Rhodes, and E. F. W. Seymour, *Proc. Phys. Soc. (London)* **B70**, 345 (1957).
- ¹¹R. V. Pound and W. D. Knight, *Rev. Sci. Instr.* **21**, 219 (1950).
- ¹²The anisotropic Knight shift is often defined as $\frac{2}{3}$ of this quantity, in which case $\nu_c = [1 + K + \frac{1}{2}K_A(3 \cos^2\theta - 1)]\nu_n$.
- ¹³H. Alloul and R. Deltour, *Phys. Rev.* **183**, 414 (1969).
- ¹⁴J. W. Searle, R. C. Smith, and S. J. Wyard, *Proc. Phys. Soc. (London)* **A74**, 491 (1959).
- ¹⁵M. Abramowitz and I. Stegun, *Handbook of Mathematical Functions* (U. S. GPO, Washington, D. C., 1964), Natl. Bur. Std. (U. S. Math.) Ser. 54, p. 319.
- ¹⁶Yu. S. Karimov and I. F. Shchegolev, *Zh. Eksperim. i Teor. Fiz.* **40**, 1289 (1960) [*Sov. Phys. JETP* **13**, 908 (1961)].
- ¹⁷D. A. Rigney and C. P. Flynn, *Phil. Mag.* **15**, 1213 (1967).
- ¹⁸R. J. Snodgrass and L. H. Bennett, *Phys. Rev.* **134**, A1295 (1964).
- ¹⁹G. Weisz, *Phys. Rev.* **149**, 504 (1966).
- ²⁰J. A. Lee and G. V. Raynor, *Proc. Phys. Soc. (London)* **B67**, 737 (1954).
- ²¹F. V. Burckbuchler and C. A. Reynolds, *Phys. Rev.* **175**, 550 (1968).
- ²²G. E. H. Reuter and E. H. Sondheimer, *Proc. Roy. Soc. (London)* **A195**, 336 (1948).
- ²³P. S. Allen and E. F. W. Seymour, *Proc. Phys. Soc. (London)* **82**, 174 (1963).
- ²⁴F. C. Thatcher, Ph.D. dissertation (University of California, Riverside, 1969) (unpublished).
- ²⁵D. E. MacLaughlin, J. D. Williamson, and J. Butterworth, *Phys. Rev. B* **4**, 60 (1971).

Magic-Angle NMR Experiments in Solids*

M. Mehring[†] and J. S. Waugh

*Department of Chemistry and Research Laboratory of Electronics,
Massachusetts Institute of Technology, Cambridge, Massachusetts 02139*

(Received 1 September 1971)

The time dependence of different interaction Hamiltonians of nuclear spins as encountered in NMR experiments where the external field is applied at the "magic angle" in the rotating frame is treated with the average Hamiltonian theory. First- and second-order correction terms of the average Hamiltonian are obtained for symmetric and antisymmetric cycles. New types of pulsed "magic-angle" experiments are treated in detail and experiments are performed to show their capability to resolve chemical shifts in solids. It is shown that such magic-angle methods, employed with applied fields of high duty factor, in principle offer advantages in the high-resolution NMR of solids over resonant multiple-pulse schemes. The problem of observing the nuclear-precession signal during applications of the strong fields is solved by "nesting" an observing cycle of low duty factor into the continuous or quasicontinuous irradiation sequence.

I. INTRODUCTION

The magnetic dipolar Hamiltonian \mathcal{H}_D of nuclei with spin I can be expressed as a scalar product of two second-rank tensor operators¹⁻⁴ representing its spatial and spin symmetry, respectively. Experiments have been performed utilizing this symmetry in which one operates on one or the other tensor in order to cancel out the dipolar Hamiltonian.

The first class of experiments involves spinning the sample^{5,6} with the rotation axis tilted by an angle θ with respect to the magnetic field H_0 , whereas in the second class, irradiation with strong

rf fields produces an effective field H_{eff} , which is tilted by an angle β with respect to H_0 .⁷⁻¹⁰ In both cases the Hamiltonian becomes time dependent in a periodic fashion with a certain period or cycle time t_c . In case the cycle time is short enough to allow coherent averaging, the Hamiltonian of the system can be replaced by an average Hamiltonian,¹⁰ expressed as a sum of different correction terms:

$$\bar{\mathcal{H}} = \bar{\mathcal{H}}^{(0)} + \bar{\mathcal{H}}^{(1)} + \bar{\mathcal{H}}^{(2)} + \dots, \quad (1a)$$

where

$$\bar{\mathcal{H}}^{(0)} = t_c^{-1} \int_0^{t_c} dt \bar{\mathcal{H}}(t),$$

$$\bar{\mathcal{C}}^{(1)} = -i(2t_c)^{-1} \int_0^{t_c} dt_2 \int_0^{t_2} dt_1 [\bar{\mathcal{C}}(t_2), \bar{\mathcal{C}}(t_1)], \quad (1b)$$

$$\begin{aligned} \bar{\mathcal{C}}^{(2)} = & -(6t_c)^{-1} \int_0^{t_c} dt_3 \int_0^{t_3} dt_2 \\ & \times \int_0^{t_2} dt_1 \{ \bar{\mathcal{C}}(t_3) \bar{\mathcal{C}}(t_2) \bar{\mathcal{C}}(t_1) \}, \end{aligned}$$

with

$$\begin{aligned} \{ \bar{\mathcal{C}}(t_3) \bar{\mathcal{C}}(t_2) \bar{\mathcal{C}}(t_1) \} = & [\bar{\mathcal{C}}(t_3), [\bar{\mathcal{C}}(t_2), \bar{\mathcal{C}}(t_1)]] \\ & + [\bar{\mathcal{C}}(t_1), [\bar{\mathcal{C}}(t_2), \bar{\mathcal{C}}(t_3)]], \quad (2) \end{aligned}$$

and \mathcal{C} stands for the corresponding Hamiltonian divided by \hbar throughout this article.

Considering the secular part of the dipolar Hamiltonian,

$$\mathcal{H}_D = - \sum_{i < j} b_{ij} (3I_{zi} I_{zj} - \vec{I}_i \cdot \vec{I}_j),$$

$$b_{ij} = \gamma^2 \hbar^{-1} r_{ij}^{-3} \frac{1}{2} (3 \cos^2 \theta_{ij}),$$

this means that in the sample-spinning experiments the average has to be taken over the time-dependent spatial part $b_{ij}(t)$, whereas in the strong-rf-field case the spin part becomes time dependent, as will be shown in Sec. IV, and has to be averaged. If the spinning angle θ fulfills the special condition

$$\cos^2 \theta_m = \frac{1}{3},$$

which is the case for the so-called "magic angle"

$$\theta_m = 54^\circ 44',$$

$\langle b_{ij} \rangle_{t_c}$ vanishes and so does the average dipolar Hamiltonian. Since the spin part of the dipolar Hamiltonian shows the same symmetry, its average vanishes if the effective field is tilted by the "magic angle" compared to H_0 .

We would like to contribute to the latter class of experiments by describing a few experiments performed by actually applying different kinds of *time-dependent* fields at the magic angle. Since strong-rf-field irradiation is much more under the experimenter's control than macroscopic manipulations of the sample such as sample spinning, these kinds of experiments have proven to be very successful in cancelling the dipolar Hamiltonian and unravelling other types of information, such as chemical-shift tensors.¹¹⁻¹³ We shall begin by showing that the application of fields at the magic angle, continuously or at least with high duty factor, offers advantages in principle over the use of trains of short pulses applied at exact resonance.

II. CONTINUOUS COHERENT AVERAGING

In the multiple-pulse line-narrowing experiments^{9,10} rf irradiation is considered to be applied only during short pulses (δ -function-pulse assumption). Since no coherent averaging is obtained

during the rf irradiation, any finite pulse width leads to a decrease in resolution in the line-narrowing experiment. To a certain degree the effect of finite pulse width can of course be compensated¹⁰; nevertheless, as short as possible a pulse is desired. Especially if one approaches very short cycle times t_c in order to reduce the leading second-order correction term $\bar{\mathcal{C}}^{(2)}$ [Eq. (1)], a very high H_1 field, i.e., very strong rf power, has to be applied.

A different way to obtain short cycle times would be to perform the experiment in such a way that coherent averaging is obtained also *during* rf irradiation. This would even allow us to apply a continuous rf field, where the cycle time is now determined by the rf field alone, thus obtaining much shorter cycle times with a given rf power or the same cycle time as in a multiple-pulse experiment with much less power. In order to observe the nuclear magnetization, the rf field can be turned off every few cycles for a few microseconds.

An experiment of this kind would be complementary to a multiple-pulse experiment, since it exhibits a high duty factor δ which is the ratio of the average rf power during a cycle to the rf power during rf irradiation. A general aspect of this fact is that, considering a given average rf power \bar{P} , the ratio of the cycle times t_c of two experiments with different duty factors δ is given by

$$(t_{c1}/t_{c2})_{\bar{P}=\text{const}} = (\delta_1/\delta_2)^{1/2}. \quad (3)$$

As an example one may consider a four-pulse experiment, which can be successfully operated with a duty factor of about 0.2 and a Lee-Goldburg (LG) experiment,⁷ where $\ell=1$, which leads to a reduction in cycle time by a factor of $\sqrt{5}$ in the LG experiment according to Eq. (3).

Since experiments with a duty factor $\delta=1$ do not allow for observing the nuclear magnetization one would like to implement for n cycles, an observing cycle containing at least one "window." This *nesting* procedure should be done in such a way that the average dipolar Hamiltonian vanishes over the *entire* cycle,

$$t_c = nt_{c1} + t_{c0},$$

where t_{c1} is the cycle time of the continuous-irradiation cycle and t_{c0} is the cycle time of the observing cycle. In case $\bar{\mathcal{C}}^{(0)}(t_{c0}) = \bar{\mathcal{C}}^{(0)}(t_{c1}) = 0$ and $\bar{\mathcal{C}}^{(1)}(t_{c0}) = \bar{\mathcal{C}}^{(1)}(t_{c1}) = 0$ the leading correction term $\bar{\mathcal{C}}^{(2)}(t_c)$ can be expressed as

$$\bar{\mathcal{C}}^{(2)}(t_c) = (nt_{c1}^3 A + t_{c0}^3 B) / (nt_{c1} + t_{c0}), \quad (4)$$

where

$$\bar{\mathcal{C}}^{(2)}(t_{c1}) = t_{c1}^2 A, \quad \bar{\mathcal{C}}^{(2)}(t_{c0}) = t_{c0}^2 B.$$

In order to estimate the efficiency of the nesting

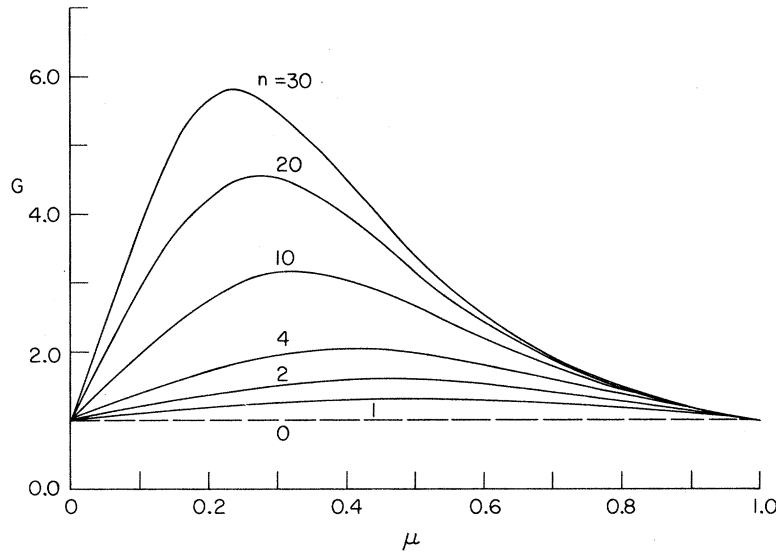


FIG. 1. Gain G in resolution due to a decrease of the second-order correction term $\bar{\mathcal{H}}^{(2)}$ vs $\mu = t_{c1}/t_{c0}$ (see text). n is the number of fast cycles per observing cycle.

procedure we assume $A \approx B$, so that Eq. (4) becomes

$$\bar{\mathcal{H}}^{(2)}(t_c) = t_{\text{eff}}^2 A, \quad (5)$$

with the effective cycle time

$$t_{\text{eff}}^2 = (nt_{c1}^3 + t_{c0}^3) / nt_{c1} + t_{c0}, \quad (6)$$

which fulfills the condition $t_{c1} \leq t_{\text{eff}} \leq t_{c0}$.

The ratio $\mu = t_{c1}/t_{c0}$ determines how much more effective in decreasing $\bar{\mathcal{H}}^{(2)}(t_c)$ the implantation of n fast cycles is compared to applying only the experimentally limited observing cycle.

In order to parametrize the gain in resolution due to a decrease in $\bar{\mathcal{H}}^{(2)}(t_c)$ obtained by the nesting procedure we introduce a gain factor

$$G = \frac{\bar{\mathcal{H}}^{(2)}(t_{c0})}{\bar{\mathcal{H}}^{(2)}(t_c)} = \frac{n\mu + 1}{n\mu^3 + 1}. \quad (7)$$

Figure 1 shows a plot of G vs μ for different numbers n of fast cycles. As one can see, there is an optimum value of μ for a given n . Thus, a considerable reduction in the second correction term of the Hamiltonian can be achieved by the implantation of fast continuous rf cycles as demonstrated in Fig. 1.

III. SYMMETRY OF CYCLES

In order to calculate the second correction term of the Hamiltonian $\bar{\mathcal{H}}^{(2)}(t_c)$ in nested cycles proposed above, it is useful to consider the behavior of the different correction terms due to the symmetry of the time-dependent Hamiltonian $\mathcal{H}(t)$ during a cycle.¹⁴⁻¹⁶ It has been shown previously¹⁵ that $\bar{\mathcal{H}}^{(1)}(t_c) = 0$ for a symmetric cycle, i. e., $\mathcal{H}(t) = \mathcal{H}(t_c - t)$. Furthermore it will be proved here that this is true also for an antisymmetric cycle $\mathcal{H}(t) = -\mathcal{H}(t_c - t)$. Thus

$$\bar{\mathcal{H}}^{(1)}(t_c) = 0 \quad \text{if} \quad \mathcal{H}(t) = \pm \mathcal{H}(t_c - t) \quad (8)$$

even though $\bar{\mathcal{H}}^{(0)}(t_c) \neq 0$ (proved in Appendix A 1).

As shown in Appendix A 2, the antisymmetric cycle has a further interesting feature, namely,

$$\bar{\mathcal{H}}^{(2)}(t_c) = 0 \quad \text{if} \quad \mathcal{H}(t) = -\mathcal{H}(t_c - t), \quad (9)$$

whereas $\bar{\mathcal{H}}^{(2)}(t_c) \neq 0$ for a symmetric cycle. But there arises a simplification in the calculation for $\bar{\mathcal{H}}^{(2)}(t_c)$ in a symmetric cycle, since

$$\bar{\mathcal{H}}^{(2)}(t_c) = \bar{\mathcal{H}}^{(2)}(\frac{1}{2}t_c) \quad \text{if} \quad \mathcal{H}(t) = \mathcal{H}(t_c - t). \quad (10)$$

Since cycles can in general be separated into a sum of a symmetric and an antisymmetric cycle it is appropriate to study the behavior of the correction terms for such a mixed-symmetry Hamiltonian, i. e.,

$$\mathcal{H}(t) = \mathcal{H}_S(t) + \mathcal{H}_A(t), \quad (11)$$

where the subscript S stands for symmetric and A stands for antisymmetric.

The second correction term $\bar{\mathcal{H}}^{(2)}(t_c)$ contains in its integrand all possible combinations of $\mathcal{H}_S(t)$ and $\mathcal{H}_A(t)$. However, since their integral vanishes if one supposes that the average Hamiltonian $\bar{\mathcal{H}}^{(0)}(t_c)$ vanishes for the symmetric and the antisymmetric part separately (see Appendix A 2), the following combinations do not contribute to $\bar{\mathcal{H}}^{(2)}(t_c)$:

$$\begin{aligned} & \{\bar{\mathcal{H}}_A(t_3)\bar{\mathcal{H}}_A(t_2)\bar{\mathcal{H}}_A(t_1)\} \quad \{\bar{\mathcal{H}}_S(t_3)\bar{\mathcal{H}}_S(t_2)\bar{\mathcal{H}}_A(t_1)\}, \\ & \{\bar{\mathcal{H}}_A(t_3)\bar{\mathcal{H}}_S(t_2)\bar{\mathcal{H}}_S(t_1)\} \quad \{\bar{\mathcal{H}}_S(t_3)\bar{\mathcal{H}}_A(t_2)\bar{\mathcal{H}}_S(t_1)\}. \end{aligned} \quad (12)$$

Other terms do not vanish and have to be evaluated separately. The symmetry relations derived in Appendix A 2 can of course be used in obtaining simpler formulas. For example, all the integrals

containing

$$\{\tilde{\mathcal{H}}_S(t_3)\tilde{\mathcal{H}}_A(t_2)\tilde{\mathcal{H}}_A(t_1)\} \text{ and } \{\tilde{\mathcal{H}}_S(t_3)\tilde{\mathcal{H}}_S(t_2)\tilde{\mathcal{H}}_S(t_1)\} \quad (13)$$

have to be evaluated only over the time $\frac{1}{2}t_c$, since they fulfill a symmetry relation, such as

$$\tilde{\mathcal{H}}^{(2)}(t_c) = \tilde{\mathcal{H}}^{(2)}(\frac{1}{2}t_c)$$

over these integrands.

On the other hand, no further simplification is possible for the integrals containing

$$\{\tilde{\mathcal{H}}_A(t_3)\tilde{\mathcal{H}}_A(t_2)\tilde{\mathcal{H}}_S(t_1)\} \text{ and } \{\tilde{\mathcal{H}}_A(t_3)\tilde{\mathcal{H}}_S(t_2)\tilde{\mathcal{H}}_A(t_1)\}, \quad (14)$$

and their integrals have to be evaluated over the full cycle time t_c .

IV. INTERACTION HAMILTONIAN IN CYCLIC rf FIELDS

A. General Discussion

With the total Hamiltonian of the spin system as a sum of an external and an internal part,

$$\mathcal{H} = \mathcal{H}_{\text{ext}} + \mathcal{H}_{\text{int}}, \quad (15)$$

we solve the equation of motion for the spin-density matrix $\rho(t)$ in the usual way¹⁰:

$$\rho(t) = L(t)\rho(0)L^\dagger(t),$$

with

$$L(t) = T \exp[-i \int_0^t dt' [\mathcal{H}_{\text{ext}}(t') + \mathcal{H}_{\text{int}}(t')]], \quad (16)$$

where T is the Dyson time-ordering operator.

In order to separate the part of the motion which is due to the external fields, we choose the following interaction representation¹⁰:

$$L(t) = L_1(t)\mathcal{L}(t),$$

where

$$L_1(t) = T \exp[-i \int_0^t dt' \mathcal{H}_{\text{ext}}(t')]$$

and

$$\mathcal{L}(t) = T \exp[-i \int_0^t dt' \tilde{\mathcal{H}}(t')], \quad (17)$$

with

$$\tilde{\mathcal{H}}(t) = L_1^{-1}(t)\mathcal{H}_{\text{int}}L_1(t).$$

As shown previously¹⁰ we consider cyclic rf fields with

$$L_1(Nt_c) = 1$$

and use the Magnus expansion

$$\mathcal{L}(t) = e^{-iNt_c\tilde{\mathcal{H}}},$$

where $\tilde{\mathcal{H}}$ is given by Eq. (1).

Again $\mathcal{H}_{\text{ext}}(t)$ may be expressed by a sum

$$\mathcal{H}_{\text{ext}}(t) = \mathcal{H}_0(t) + \mathcal{H}_R(t), \quad (18)$$

where, for example, but not necessarily, $\mathcal{H}_0(t)$ may be thought of as the Zeeman interaction and $\mathcal{H}_R(t)$ as the interaction due to the rf field.

As with Eq. (18), the time evolution operator $L_1(t)$, which is due to the external fields, may be separated into a part which is due to the main interaction $L_0(t)$ and a part which describes the motion in that arbitrarily chosen representation:

$$L_1(t) = L_0(t)L_R(t),$$

where

$$L_0(t) = T \exp[-i \int_0^t dt' \mathcal{H}_0(t')]$$

and

$$L_R(t) = T \exp[-i \int_0^t dt' \tilde{\mathcal{H}}_R(t')],$$

with

$$\tilde{\mathcal{H}}_R(t) = L_0^{-1}(t)\mathcal{H}_R(t)L_0(t).$$

If

$$\mathcal{H}_0 = -\omega I_z,$$

the above more general procedure corresponds to the "rotating-frame" representation.

$L_R(t)$ again may be written as a product of operators if this is suitable, thus separating the different transformations. What one wishes to establish is of course a simple expression for $L_1(t)$, so that the different types of transformations can easily be carried out. To clarify this point we choose the following external-field Hamiltonian:

$$\mathcal{H}_{\text{ext}} = -\omega_0 I_z + 2\omega_1 I_x \cos \omega t, \quad (20)$$

where

$$\omega_0 = \gamma H_0 \text{ and } \omega_1 = \gamma H_1.$$

According to Eq. (20), $L_1(t)$ can be written as

$$L_1(t) = e^{i\omega I_z t} L_R(t), \quad (21)$$

where $L_R(t)$ is defined in Eq. (19) with

$$\tilde{\mathcal{H}}_R(t) = (\omega - \omega_0) I_z + \omega_1 I_x + \omega_1 (I_x \cos 2\omega t + I_y \sin 2\omega t). \quad (22)$$

If the time dependence of $\tilde{\mathcal{H}}_R(t)$ with the frequency 2ω is neglected [which corresponds to expressing $\tilde{\mathcal{H}}_R(t)$ by its average Hamiltonian $\tilde{\mathcal{H}}_R^{(0)}$], $L_1(t)$ can be written as

$$L_1(t) = \exp(i\omega I_z t) \exp[-i[(\omega - \omega_0)I_z + \omega_1 I_x]t]. \quad (23)$$

According to the above rules, $L_R(t)$ may again be expressed by a product of operators as

$$\exp[-i[(\omega - \omega_0)I_z + \omega_1 I_x]t] = e^{-i\beta I_y} e^{-i\omega_e I_z t} e^{i\beta I_y},$$

where

$$\beta = \tan^{-1} \omega_1 / (\omega - \omega_0)$$

and

$$\omega_e^2 = (\omega - \omega_0)^2 + \omega_1^2. \quad (24)$$

In this sense, the application of an rf field with arbitrary phase can be represented by a rotation about a certain axis in the rotating frame as follows:

$$L_R(t) = e^{-i\gamma(t)\vec{n} \cdot \vec{I}}, \quad (25)$$

where $\gamma(t) = \omega_e t$ and

$$\vec{n} = n_x \vec{i} + n_y \vec{j} + n_z \vec{k}, \quad \vec{I} = I_x \vec{i} + I_y \vec{j} + I_z \vec{k},$$

with the unit vectors \vec{i} , \vec{j} , and \vec{k} defined in the rotating frame. If the time dependence of $\mathcal{H}_R(t)$ is not ignored in Eq. (22), then the first-order correction term, according to Eq. (1), leads to¹⁷

$$\overline{\mathcal{H}_R}^{(1)}(T) = \frac{1}{4} \frac{\omega_1^2}{\omega} I_x - \frac{1}{2} \frac{\omega_1(\omega - \omega_0)}{\omega} I_x, \quad (26)$$

where $T = 2\pi/\omega$, so that the Hamiltonian is averaged over one cycle of the applied rf signal ω . At resonance, $\omega = \omega_0$, this first-order correction to the average Hamiltonian is called the Bloch-Siegert shift.¹⁸

Neglecting this shift in the further discussion, $L_R(t)$ can be written in general as a product of operators:

$$L_R(t) = R_x(\alpha) R_y(\beta) R_z(\gamma(t)) R_y^{-1}(\beta) R_x^{-1}(\alpha), \quad (27)$$

where

$$R_x(\alpha) = e^{-i\alpha I_x}, \quad R_y(\beta) = e^{-i\beta I_y},$$

and the angles (α, β, γ) are the Eulerian angles which describe the transformation from the "rotating frame" to the double-tilted rotating (DTR) frame. Thus the whole problem of applying an external field to the spins I is written as a product of operations on the internal Hamiltonian:

$$L_1(t) = L_0(t) L_R(t) \\ = R_x^{-1}(\omega t) R_x(\alpha) R_y(\beta) R_z(\gamma(t)) R_y^{-1}(\beta) R_x^{-1}(\alpha), \quad (28)$$

which leads to a simple algebra when evaluating the time dependence of the Hamiltonian $\mathcal{H}_{\text{int}}(t)$.

In the discussion of the internal Hamiltonian \mathcal{H}_{int} we encounter two different types of Hamiltonian, those expressed by first-rank tensor operators T_{1M} or by second-rank tensor operators T_{2M} of the spin variables. As an example we can write the chemical-shift Hamiltonian as

$$\mathcal{H}_C = \sum_j \sum_{M=-1}^{+1} (-1)^M S_{1,-M} T_{1M}, \quad (29)$$

where

$$T_{10} = I_{zj},$$

$$T_{1,\pm 1} = \mp (1/\sqrt{2}) I_{\pm j}$$

and

$$S_{1,0} = \sigma_{zz}^{(j)} \omega_0,$$

$$S_{1,\pm 1} = \mp (1/\sqrt{2}) (\sigma_{xx}^{(j)} \pm i\sigma_{xy}^{(j)}) \omega_0.$$

In a similar way we can express the dipolar Hamiltonian²

$$\mathcal{H}_D = - \sum_{i < j} \sum_{M=-2}^{+2} (-1)^M B_{2,-M} T_{2M}, \quad (30)$$

where

$$T_{20} = (\frac{2}{3})^{1/2} (3I_{zi} I_{zj} - I_i I_j),$$

$$T_{2\pm 1} = \mp (I_{zi} I_{\pm j} + I_{zj} I_{\pm i}),$$

$$T_{2\pm 2} = I_{\pm i} I_{\pm j},$$

and

$$B_{2,-M} = (\frac{6}{5} \pi)^{1/2} \gamma^2 \hbar^{-3} r_{ij}^{-3} Y_{2,-M}^{(i,j)},$$

with the spherical harmonics $Y_{2,-M}$.

The quadrupole Hamiltonian and the pseudo-dipolar Hamiltonian assume the same form as the dipolar Hamiltonian in Eq. (30), where only the factor $B_{2,-M}$ has a different form than in Eq. (30). Since we discuss operations on the spin variables of the internal Hamiltonians only, everything to be derived for the dipolar Hamiltonian is of course true also for those others.

Operations to be considered are of the form

$$L_1^{-1}(t) T_{jM} L_1(t) = \sum_{M'=-j}^{+j} T_{jM'} D_{M'M}^{(j)}(\alpha, \beta, \gamma), \\ j = 1 \text{ or } 2 \quad (31)$$

where

$$D_{M'M}^{(j)}(\alpha, \beta, \gamma) = \langle jM' | L_1^{-1}(\alpha, \beta, \gamma) | jM \rangle.$$

By using Eqs. (28) and (31) we can write

$$L_1^{-1}(t) T_{j'M} L_1(t) = T_{j'M}^R e^{-iM\omega t}, \quad (32)$$

where

$$T_{j'M}^R = L_R^{-1}(t) T_{j'M} L_R(t). \quad (33)$$

So far no separation of the Hamiltonian into secular and nonsecular parts has been made. If we now truncate the Hamiltonian, meaning that we neglect oscillating terms with the frequency ω and 2ω , where ω is close to the Larmor frequency, we obtain for the truncated tensor operator T_{j0}^R :

$$T_{j0}^R = [L_R^{-1}(t) T_{jM} L_R(t)]_{M=0} \quad (34)$$

and, according to Eq. (31),

$$T_{j0}^R = \sum_{M'} T_{jM'} D_{M'0}^{(j)}(\alpha, \beta, \gamma), \quad (35)$$

where

$$D_{M'0}^{(j)} = \langle jM' | L_R^{-1}(\alpha, \beta, \gamma) | j0 \rangle.$$

$D_{M'0}^{(j)}(\alpha, \beta, \gamma)$ can be easily evaluated for any set of (α, β, γ) by making use of the matrix elements

$$d_{M^*M}^{(j)}(\beta) = \langle jM^* | e^{-iB I_y} | jM \rangle \quad (36)$$

as given in any standard text. If we use the notation of $L_R(t)$ as given by Eq. (28), which represents the interaction in the rotating frame, we obtain

$$D_{M^*0}^{(j)}(\alpha, \beta, \gamma) = e^{-iM^*\alpha} \sum_M d_{M^*M}^{(j)}(\beta) d_{0M}^{(j)}(\beta) e^{-iM^*\gamma}, \quad (37)$$

where the symmetry relations of the $d_{M^*M}^{(j)}(\beta)$ have been used.

It is very convenient to express the interaction in the DTR frame, with

$$L_R^{\text{DTR}}(t) = R_z(\gamma) R_y^{-1}(\beta) R_z^{-1}(\alpha), \quad (38)$$

which leads to

$$D_{M^*0}^{(j)}(\alpha, \beta, \gamma) = d_{0M^*}^{(j)}(\beta) e^{-iM^*\gamma}. \quad (39)$$

Combining Eqs. (32)–(39), T_{j0} can be most conveniently expressed by

$$T_{j0} = \sum_M T^{(M)} e^{-iM^*\gamma}, \quad (40)$$

where

$$T^{(M)} = \sum_{M^*} T_{jM^*} d_{M^*M}^{(j)}(\beta) d_{0M}^{(j)}(\beta) e^{-iM^*\alpha}$$

in the rotating frame or

$$T^{(M)} = T_{jM} d_{0M}^{(j)}(\beta) \quad (41)$$

in the DTR frame.

We arrive at very simple expressions for the interaction Hamiltonians in strong rf fields with the time-dependent chemical-shift Hamiltonian as

$$\tilde{\mathcal{H}}_c(t) = \sum_{M=-1}^{+1} \mathcal{H}(M) e^{-iM^*\gamma(t)}, \quad (42)$$

where

$$\mathcal{H}(M) = \omega_0 \sum_i \sum_{M^*=-1}^{+1} \sigma_{zzi} T_{1M^*} d_{M^*M}^{(1)}(\beta) d_{0M}^{(1)}(\beta) e^{-iM^*\alpha}$$

in the rotating frame or

$$\mathcal{H}(M) = \omega_0 \sum_i \sigma_{zzi} T_{1M} d_{0M}^{(1)}(\beta)$$

in the DTR frame, and the dipolar Hamiltonian as

$$\tilde{\mathcal{H}}_D(t) = \sum_{M=-2}^{+2} \mathcal{H}(M) e^{-iM^*\gamma(t)}, \quad (43)$$

where

$$\mathcal{H}(M) = - \sum_{i < j} \sum_{M^*=-2}^{+2} B_{2,0}^{(ij)} T_{2M^*} d_{M^*M}^{(2)}(\beta) d_{0M}^{(2)}(\beta) e^{-iM^*\alpha}$$

in the rotating frame or

$$\mathcal{H}(M) = - \sum_{i < j} B_{2,0}^{(ij)} T_{2M} d_{0M}^{(2)}(\beta)$$

in the DTR frame.

Note that the basic expression for the time-dependent interaction Hamiltonians, Eqs. (42) and (43), is the same except for the range of the index M ; thus, they can be treated most generally in the same fashion. Differences occur only because of

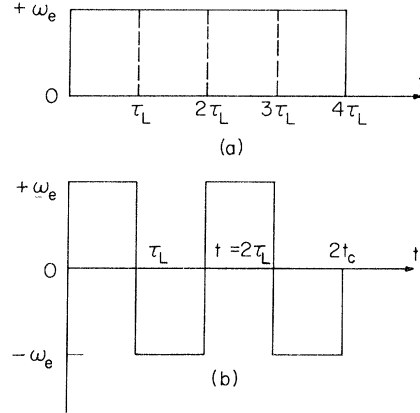


FIG. 2. Timing of the effective frequency ω_e for (a) the LG cycle with the cycle time τ_L and (b) the FFLG cycle with the cycle time $2\tau_L$.

the different symmetry of the Hamiltonians expressed by the $d_{M^*M}^{(j)}$.

B. LG Experiment and its Modification

In the LG experiment a constant rf field with the frequency $\omega \neq \omega_0$, where ω_0 is the Larmor frequency, is applied to the spin system as indicated in Fig. 2(a). With the general time-dependent interaction Hamiltonian in a strong rf field [Eqs. (42) and (43)]

$$\tilde{\mathcal{H}}(t) = \sum_M \mathcal{H}(M) e^{-iM\omega_e t}, \quad (44)$$

where ω_e is given by the effective field H_{eff} in the rotating frame, we obtain for the average Hamiltonian, Eq. (1), over one LG cycle, $\tau_L = 2\pi/\omega_e$, immediately

$$\overline{\mathcal{H}}^{(0)} = (1/\tau_L) \int_0^{\tau_L} dt' \tilde{\mathcal{H}}(t') = \mathcal{H}(0). \quad (45)$$

According to Eq. (43) this leads for the dipolar Hamiltonian in the DTR frame to

$$\overline{\mathcal{H}}_D^{(0)} = - \sum_{i < j} B_{2,0}^{(ij)} d_{00}^{(2)}(\beta) T_{20}, \quad (46)$$

where

$$d_{00}^{(2)}(\beta) = P_2(\cos\beta),$$

from which it follows that $\overline{\mathcal{H}}_D^{(0)}$ vanishes if β is the magic angle β_m with $\cos^2\beta_m = \frac{1}{3}$.

For the average chemical-shift Hamiltonian in the DTR frame we obtain, using Eqs. (42) and (45),

$$\overline{\mathcal{H}}_c^{(0)} = \omega_0 \sum_i \sigma_{zzi} T_{10} d_{00}^{(1)}(\beta), \quad (47)$$

where

$$d_{00}^{(1)}(\beta) = \cos\beta.$$

In order to calculate the first correction term to

the average Hamiltonian, we use the above-derived symmetry relations and utilize the fact that $\overline{\mathcal{H}}(t)$ of Eqs. (42) and (43) can be written as a sum of a symmetric and an antisymmetric Hamiltonian:

$$\overline{\mathcal{H}}(t) = \mathcal{H}_S(t) + \mathcal{H}_A(t) ,$$

where

$$\mathcal{H}_S(t) = \sum_M \mathcal{H}(M) \cos M\omega_e t \quad (48)$$

and

$$\mathcal{H}_A(t) = i \sum_M \mathcal{H}(M) \sin M\omega_e t .$$

Due to the derived symmetry relations (Appendix A 1) the part of the first-order correction term of the Hamiltonian, which contains the commutators

$$[\mathcal{H}_S(t_2), \mathcal{H}_S(t_1)] \text{ and } [\mathcal{H}_A(t_2), \mathcal{H}_A(t_1)] ,$$

vanishes, thus leaving only the terms with the integrands

$$[\mathcal{H}_A(t_2), \mathcal{H}_S(t_1)] \text{ and } [\mathcal{H}_S(t_2), \mathcal{H}_A(t_1)] ,$$

which leads immediately to:

$$\overline{\mathcal{H}}^{(1)} = - \frac{\tau_L}{2\pi} \sum_{M \neq 0} \frac{1}{M} \{ 2[\mathcal{H}(M), \mathcal{H}(0)] + \frac{1}{2} [\mathcal{H}(-M), \mathcal{H}(M)] \} . \quad (49)$$

This, together with Eqs. (42) and (43), allows one to calculate the first-order correction for any angle β in the LG experiment.

In the case of the magic-angle condition $\beta = \beta_m$, $\overline{\mathcal{H}}(0)$ vanishes for the dipolar interaction and Eq. (49) is consistent with the result as cited in Ref. 10.

The first-order correction term to the chemical-shift average Hamiltonian, Eq. (47), is easily obtained from Eq. (49) as

$$\overline{\mathcal{H}}_c^{(1)} = - \frac{t_c}{2\pi} \omega_0^2 \sum_i \sigma_{zzi}^2 [\sin 2\beta I_{xi} + (\frac{1}{2} \sin^2 \beta) I_{zi}] . \quad (50)$$

This correction term to the "ordinary scaling factor" $\cos \beta$ for the chemical shift in magic-angle experiments is very small if $\omega_0 \sigma_{22} t_i / 2\pi \ll 1$, which is usually the case.

The first-order correction term to the average dipolar Hamiltonian, however, is rather big, thus leading to a fast decay or broad lines in the LG experiment, which makes the LG experiment not very useful for line-narrowing experiments, where one wants to observe small chemical shifts in solids.¹⁰⁻¹² There is still, of course, the cross term between the chemical shift and dipolar Hamiltonians in the first correction term to be considered, which is easily evaluated, according to Eq. (49), but is of no further interest here. However, the first correction term can be made to vanish identically if one produces a symmetric or antisymmetric cycle as shown in Sec. II. This can

be utilized in the so-called flip-flop Lee-Goldburg (FFLG) experiment, where the phase of ω_e is switched by π after each 2π cycle [see Fig. 2(b)].

According to Eqs. (42) and (43), $\mathcal{H}(t)$ is given by

$$\begin{aligned} \tilde{\mathcal{H}}(t) &= \sum_M \mathcal{H}(M) e^{-iM\omega_e t} & \text{for } 0 \leq t < \tau_L , \\ \tilde{\mathcal{H}}(t) &= \sum_M \mathcal{H}(M) e^{-iM\omega_e(t-\tau_L)} & \text{for } \tau_L \leq t \leq t_c , \end{aligned} \quad (51)$$

where

$$t_c = 2\tau_L, \quad \omega_e \tau_L = 2\pi .$$

It follows immediately that

$$\overline{\mathcal{H}}^{(0)} = \mathcal{H}(0) ,$$

as in the LG experiment. Furthermore, it is evident that $\overline{\mathcal{H}}(t)$ is symmetric, which leads to

$$\overline{\mathcal{H}}^{(1)} \equiv 0$$

independent of the tilting angle β and which type of interaction Hamiltonian is considered. This indicates the value of the FFLG experiment for line-narrowing purposes.

If the magic-angle condition is fulfilled, the leading correction term is $\overline{\mathcal{H}}^{(2)}$, which can be evaluated using the symmetry relations (Appendix A 2) as follows: Since the interaction Hamiltonian $\mathcal{H}(t)$ in the FFLG experiment is symmetric, we only need to evaluate $\overline{\mathcal{H}}^{(2)}$ over half the cycle time, namely,

$$\overline{\mathcal{H}}^{(2)}(t_c) = \overline{\mathcal{H}}^{(2)} \frac{1}{2} t_c .$$

Thus, $\overline{\mathcal{H}}^{(2)}$ in the FFLG experiment is the same as in the LG experiment.

Again we express the time-dependent interaction Hamiltonian $\mathcal{H}(t)$ as a sum of a symmetric and an antisymmetric part. Using the symmetry rules established in Appendix A 2, we find

$$\begin{aligned} \overline{\mathcal{H}}^{(2)}(t_c) &= - \frac{\tau_L^2}{48\pi^3} \sum_{M_3 M_2 M_1 \neq 0} \{ \mathcal{H}(M_3) \mathcal{H}(M_2) \mathcal{H}(M_1) \} \\ &\quad \times \Delta^F(M_3 M_2 M_1) , \end{aligned} \quad (52)$$

where the parameters $\Delta^F(M_3 M_2 M_1)$ are numbers which depend on M_3 , M_2 , M_1 , and are given in Appendix B 1.

Even though the FFLG experiment seems to be the ideal magic-angle experiment theoretically, the major drawback in practice is that the magnetization can be observed only after a number of FFLG cycles at the end of the rf burst, thus measuring the decay point by point. In Sec. IV C we shall discuss possibilities for overcoming this obstacle.

C. Six-Pulse Experiment with Finite Pulse Width

The six-pulse experiment¹⁰ [see Fig. 3(a)] can be thought of as a stepwise FFLG experiment, where after every 120° rotation, which is produced by each pulse P_i of width τ_p , a window of width τ_w is applied

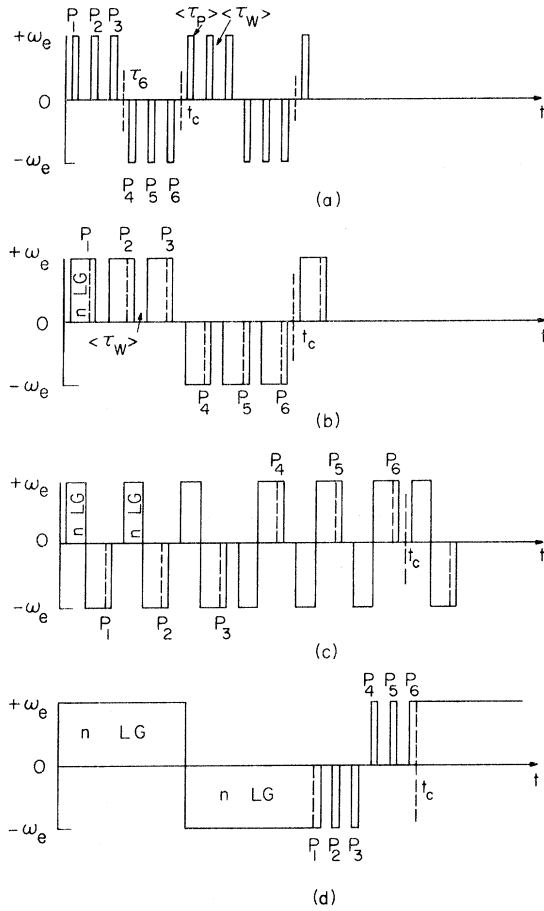


FIG. 3. Timing of the effective frequency ω_e for different types of magic-angle experiments: (a) six-pulse experiment; (b) nested-cycle type I with n -fold LG cycle; (c) nested-cycle type I with n -fold FFLG cycle; (d) nested-cycle type II where τ_p is the pulse width corresponding to a 120° rotation, τ_w is the width of the window (see text).

in order to observe the magnetization.

The interaction Hamiltonian again can be written according to Eqs. (42) and (43) with $\gamma(t) = \omega_e t P_i(t)$ during the pulses i , and $\gamma(t) = \pm \frac{2}{3} \pi k$, $k = 1, 2, \dots, 6$ during the windows, where the + holds for $k = 1, 2, 3$ and the - for $k = 4, 5, 6$. Thus the magnetization is precessing stepwise during the windows ("precessing window"). Using the relations derived in Secs. IVA and IVB, a straightforward calculation shows that

$$\bar{\mathcal{H}}^{(0)} = \mathcal{H}(0) \quad \text{and} \quad \bar{\mathcal{H}}^{(1)} = 0,$$

as in the FFLG experiment. Thus finite pulse width causes no problems in the six-pulse experiment as it does, for example, in other multiple-pulse experiments.

The second correction term $\bar{\mathcal{H}}^{(2)}(t)$ for the six-pulse experiment under the δ -function-pulse as-

sumption was derived in Ref. 10. In the case of finite pulse width it is far more complicated, but can be readily obtained by using the symmetry relations, as derived in Sec. III.

Again symmetry allows us to consider only half of the cycle, since $\bar{\mathcal{H}}(t)$ is symmetric. Assuming the magic-angle condition $\beta = \beta_m$, we obtain

$$\begin{aligned} \bar{\mathcal{H}}^{(2)} = & -\frac{\tau_6}{6} \sum_{M_3 M_2 M_1 \neq 0} \{ \mathcal{H}(M_3) \mathcal{H}(M_2) \mathcal{H}(M_1) \} \\ & \times \left[\kappa^3 \Delta^A(M_3 M_2 M_1) + \frac{3}{2\pi} \kappa^2 \lambda \Delta^B(M_3 M_2 M_1) \right. \\ & \left. + \left(\frac{3}{2\pi} \right) \lambda^2 \kappa \Delta^C(M_3 M_2 M_1) \right. \\ & \left. + \left(\frac{3}{2\pi} \right)^3 \pi \lambda^3 \Delta^F(M_3 M_2 M_1) \right], \quad (53) \end{aligned}$$

where $\tau_6 = \frac{1}{2} t_c$, $\kappa = \tau_w / \tau_6$, $\lambda = \tau_p / \tau_6$, $\kappa + \lambda = \frac{1}{3}$, and the parameters $\Delta^A(M_3 M_2 M_1)$, etc., are numbers depending on M_3 , M_2 , M_1 which are given in Appendix B2. The first part in Eq. (55), which contains $\Delta^A(M_3 M_2 M_1)$, corresponds to the δ -function pulse-assumption ($\tau_p \rightarrow 0$), whereas the last part [$\Delta^F(M_3 M_2 M_1)$] corresponds to the FFLG experiment ($\tau_w \rightarrow 0$). Equation (55) allows one to evaluate $\bar{\mathcal{H}}^{(2)}$ for any pulse-width-to-window-width ratio.

V. NESTED CYCLES

A. Type I (Precessing Window)

Figure 3(b) shows the field timing of the precessing-window type-I nested cycle, where an LG cycle is attached to each pulse of a six-pulse experiment or, the other way around, a six-pulse experiment is implanted into a FFLG experiment. Thus, this experiment is expected to show the combined features of the FFLG experiment and the six-pulse experiment.

The interaction Hamiltonian $\bar{\mathcal{H}}(t)$ can be expressed according to Eqs. (42) and (43), with

$$\gamma(t) = \omega_e t P_i(t) \quad (54)$$

during rf irradiation and

$$\gamma(t) = \pm (n + \frac{1}{3} k) 2\pi$$

during the windows where the sign is + if $k = 1, 2, 3$ and - if $k = 4, 5, 6$.

The interaction Hamiltonian $\bar{\mathcal{H}}(t)$ is again symmetric, and the average Hamiltonians are readily obtained as

$$\bar{\mathcal{H}}^{(0)} = \mathcal{H}(0),$$

which vanishes if the magic-angle condition is met, and

$$\bar{\mathcal{H}}^{(1)} = 0,$$

independent of the fulfillment of the magic-angle

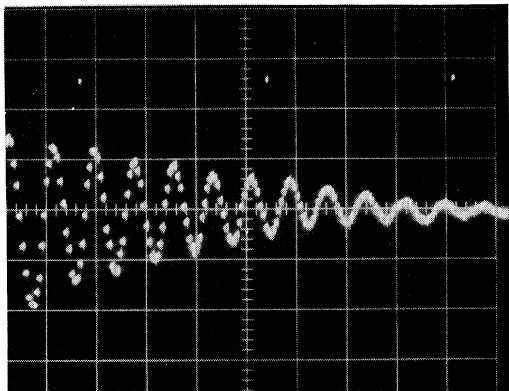


FIG. 4. Decay of F^{19} in CaF_2 as observed in a nested-cycle type-I experiment. Horizontal: $50 \mu\text{sec}/\text{point}$, window width $\tau_w = 4.5 \mu\text{sec}$, cycle time $t_c = 85 \mu\text{sec}$. The decay time is approximately 5 msec, corresponding to a linewidth of 68 Hz.

condition.

The second correction term $\overline{\mathcal{K}}^{(2)}$ can be obtained as in the six-pulse experiment by using the symmetry relations. As shown in Appendix C 1, we obtain

$$\overline{\mathcal{K}}_{S1}^{(2)} = [1/(1+m)] \overline{\mathcal{K}}_6^{(2)}, \quad (55)$$

where $m = n\tau_L/(\tau_w + \tau_p)$. Equation (55) indicates the advantage of the nested cycle compared to an ordinary six-pulse experiment. In a practical case, where, for example, $\tau_L = 6 \mu\text{sec}$, $\tau_p = 2 \mu\text{sec}$, $\tau_w = 4 \mu\text{sec}$, one finds $m = n$, i. e., the increase in resolution due to $\overline{\mathcal{K}}^{(2)}$ is equal to $n+1$, where n is the number of implanted LG cycles.

Even in a simple case, where $n=1$, the gain in resolution may be appreciable if other effects such as phase transients, etc., contribute more to the

linewidth in multiple-pulse experiments than the second correction term. For example, the phase-transient effect, which occurs during the rise and the fall time of the pulses, is proportional to the number of pulse edges per unit time. Since the number of pulse edges per time is considerably smaller in nested-cycle experiments, a gain in resolution is expected.

Experiments were performed using a tilted-coil arrangement and a video pulser as described in Ref. 19. The magnetization was sampled every cycle in one of the windows, digitized, and stored. Figure 4 shows the off-resonance decay in CaF_2 , which corresponds to a linewidth of about 68 Hz, indicating that the coherent averaging in this experiment is quite effective. Figure 5 shows a plot of the beat frequency during the rf burst vs magnetic field offset and demonstrates the expected $1/\sqrt{3}$ scaling factor according to Eq. (47).

In order to prove that small chemical shifts can actually be resolved, Fig. 6 shows the power spectrum of a decay obtained from a tetrafluoroethylene/per fluoromethylvinyl ether copolymer (TFE/PFMVE) sample. The OCF_3 peak and the broad CF_2 line are very well separated. The shift difference of the peaks equals 4.25 kHz at 54 MHz, which corresponds to 77 ppm as reported in Ref. 20. Figure 6 also indicates that no further resolution can be obtained since the sharp line exhibits the same width as the $T_{1\rho}$ spectrum at zero frequency. Thus the resolution obtained is $T_{1\rho}$ limited⁸ in this sample.

Since the first correction term $\overline{\mathcal{K}}^{(1)}$ in the LG cycle [Eq. (49)] leads to a decay after a certain time, it is not advisable to increase the number n of LG cycles in the nested-cycle type I arbitrarily. It is suggested instead to implant n FFLG cycles,

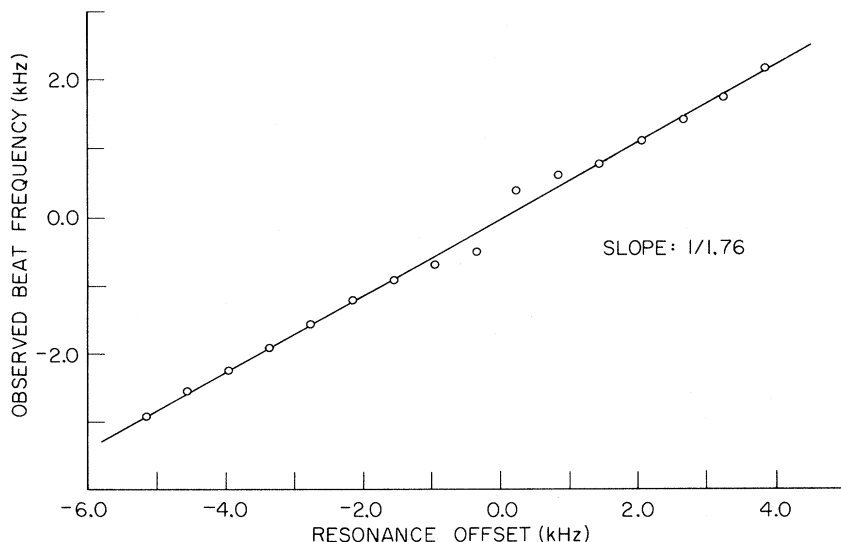


FIG. 5. Resonance offset shift of F^{19} in CaF_2 as observed in the nested-cycle type-I experiment. The slope is close to the expected value of $1/\sqrt{3}$.

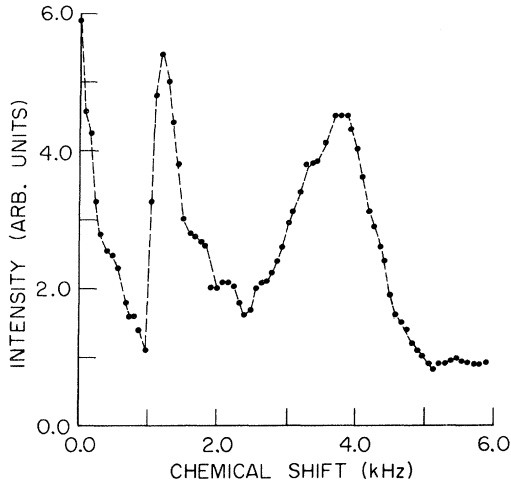


FIG 6. Power spectrum of F^{19} in TFE/PMVE obtained in a nested-cycle type-I experiment at 54 MHz.

rather than n LG cycles [Fig. 3(c)].

The average Hamiltonian and its first correction term are the same as before, i. e., coherent averaging of the interaction Hamiltonian is assumed, whereas we obtain for the second correction $\bar{\mathcal{H}}^{(2)}$ a similar result, namely,

$$\bar{\mathcal{H}}_{SI}^{(2)} = [1/(1+2m)]\bar{\mathcal{H}}_6^{(2)}, \quad (56)$$

where m is given in Eq. (55).

B. Type II (Observing Cycles)

Another possibility for constructing a nested cycle is presented in Fig. 3(d). An n -fold FFLG experiment is followed by an observing cycle in order to observe the magnetization. The average Hamiltonian and the first-order correction term are not altered compared to the cycles described above; however, the number of pulse edges per time is considerably reduced.

The second correction term $\bar{\mathcal{H}}^{(2)}$ can be expressed in terms of its six-pulse counterpart as

$$\bar{\mathcal{H}}_{SI}^{(2)} = \frac{n+M^3}{nM^2+M^3} \bar{\mathcal{H}}_6^{(2)}, \quad (57)$$

where

$$M = \tau_6/\tau_L = 1 + 3\tau_w/\tau_L$$

and under the assumption that $\bar{\mathcal{H}}_6^{(2)} = \bar{\mathcal{H}}_L^{(2)}$ for the same cycle time (see Appendix C 2). An experiment of this type was considered in Sec. II when calculating the effect of nesting. Therefore, the factor in Eq. (57) can be conveniently expressed as a "nesting gain,"

$$G = (nM^2 + M^3)/(n + M^3), \quad (58)$$

which accounts for the gain in resolution due to the

decrease in $\bar{\mathcal{H}}^{(2)}$. In practical cases, where $M = 3$ for $n = 10$, a gain $G \sim 3$ is obtained. Of course many other cycles can be invented, by permutation of the ones described here, but there is no need to discuss this further.

ACKNOWLEDGMENTS

We are indebted to R. G. Griffin, A. Pines, W.-K. Rhim, and M. Gibby for continuing valuable conversation. Special thanks are due to J. D. Ellett who designed some of the cards used for generating the pulse program.

APPENDIX A

1. First Correction Term

The first correction term $\bar{\mathcal{H}}^{(1)}(t_c)$, Eq. (1b), can be written as

$$\bar{\mathcal{H}}^{(1)}(t_c) = -i(2t_c)^{-1} \int_0^{t_c} dt_2 G(t_2), \quad (A1)$$

where

$$G(t_2) = \int_0^{t_2} dt_1 [\bar{\mathcal{H}}(t_2), \bar{\mathcal{H}}(t_1)].$$

Expressing the symmetry of the Hamiltonian $\bar{\mathcal{H}}(t)$ by a symmetry parameter P_i , we can write

$$\bar{\mathcal{H}}(t_i) = P_i \bar{\mathcal{H}}(t_c - t_i), \quad (A2)$$

where $P_i = +1$ or -1 depending on whether $\bar{\mathcal{H}}(t_c)$ is symmetric or antisymmetric.

With $t'_i = t_c - t_i$, $G(t_2)$ can be expressed as

$$G(t_2) = P_{12} \int_0^{t_2} dt_1 [\bar{\mathcal{H}}(t'_2), \bar{\mathcal{H}}(t'_1)], \quad (A3)$$

where $P_{12} = P_1 P_2$, which leads, using simple algebra, to

$$G(t_2) = P_{12} \int_0^{t_c} dt'_1 [\bar{\mathcal{H}}(t'_2), \bar{\mathcal{H}}(t'_1)] - P_{12} G(t'_2). \quad (A4)$$

The integral over the first part in Eq. (A4) vanishes in Eq. (A1), since

$$\int_0^{t_c} dt'_2 \bar{\mathcal{H}}(t'_2) = \int_0^{t_c} dt'_1 \bar{\mathcal{H}}(t'_1),$$

which leads, together with Eq. (A1), to

$$\bar{\mathcal{H}}^{(1)}(t_c) = -P_{12} \bar{\mathcal{H}}^{(1)}(t_c). \quad (A5)$$

Thus $\bar{\mathcal{H}}^{(1)}(t_c) = 0$ if $P_{12} = +1$, which is the case whether $\bar{\mathcal{H}}(t)$ is symmetric ($P_1 = P_2 = +1$) or antisymmetric ($P_1 = P_2 = -1$). In general,

$$\bar{\mathcal{H}}^{(1)}(t_c) = 0 \text{ if } G(t_2) = -G(t'_2) \quad (A6)$$

and

$$\bar{\mathcal{H}}^{(1)}(t_c) = \bar{\mathcal{H}}^{(1)} \frac{1}{2} t_c \text{ if } G(t_2) = G(t'_2). \quad (A7)$$

2. Second Correction Term

The second correction term $\bar{\mathcal{H}}^{(2)}(t_c)$ in Eq. (1b) can be written as

$$\bar{\mathcal{H}}^{(2)}(t_c) = -i(6t_c)^{-1} \int_0^{t_c} dt_3 F(t_3), \quad (\text{A8})$$

where

$$F(t_3) = \int_0^{t_3} dt_2 \int_0^{t_2} dt_1 \{ \bar{\mathcal{H}}(t_3) \bar{\mathcal{H}}(t_2) \bar{\mathcal{H}}(t_1) \}.$$

Using the symmetry parameter P_i as in Appendix A1, $F(t_3)$ can be expressed as

$$F(t_3) = P_{123} \int_0^{t_3} dt_2 \int_0^{t_2} dt_1 \{ \bar{\mathcal{H}}(t_3) \bar{\mathcal{H}}(t_2) \bar{\mathcal{H}}(t_1) \}, \quad (\text{A9})$$

where $P_{123} = P_1 P_2 P_3$, which leads, using simple algebra, to

$$\begin{aligned} F(t_3) = & P_{123} [\{ \bar{\mathcal{H}}(t_3) \bar{\mathcal{H}}^{(0)}(t_c) \bar{\mathcal{H}}^{(0)}(t_c) \} t_c^2 \\ & - \int_0^{t_3} dt'_2 \{ \bar{\mathcal{H}}(t'_2) \bar{\mathcal{H}}(t'_2) \bar{\mathcal{H}}^{(0)}(t_c) \} t_c \\ & - \int_0^{t_c} dt'_2 \int_0^{t'_2} dt'_1 \{ \bar{\mathcal{H}}(t'_2) \bar{\mathcal{H}}(t'_1) \bar{\mathcal{H}}(t'_1) \} + F(t'_3)] . \end{aligned} \quad (\text{A10})$$

Analogous to Eqs. (A6) and (A7), it is easily shown that

$$\bar{\mathcal{H}}^{(2)}(t_c) = 0 \quad \text{if } F(t_3) = -F(t'_3) \quad (\text{A11})$$

and

$$\bar{\mathcal{H}}^{(2)}(t_c) = \bar{\mathcal{H}}^{(2)}(\frac{1}{2}t_c) \quad \text{if } F(t_3) = F(t'_3).$$

Thus we distinguish the different cases of Eq. (A10) where Eqs. (A11) are fulfilled.

In the case $\bar{\mathcal{H}}^{(0)}(t_c) = 0$ and $P_{12} = 1$ the first three terms in Eq. (A10) vanish, leading to

$$F(t_3) = P_{123} F(t'_3). \quad (\text{A12})$$

In this case

$$\bar{\mathcal{H}}^{(2)}(t_c) = 0 \quad \text{if } P_{123} = -1$$

and

$$\bar{\mathcal{H}}^{(2)}(t_c) = \bar{\mathcal{H}}^{(2)}(\frac{1}{2}t_c) \quad \text{if } P_{123} = +1.$$

It can be further proved that the condition $\bar{\mathcal{H}}^{(0)}(t_c) = 0$ is not necessary. According to Eqs. (A8) and (A10), one can write

$$\begin{aligned} \bar{\mathcal{H}}^{(2)}(t_c) = & i(6t_c)^{-1} P_{123} \\ & \times [\int_0^{t_c} dt'_3 \int_0^{t'_3} dt'_2 \{ \bar{\mathcal{H}}(t'_3) \bar{\mathcal{H}}(t'_2) \bar{\mathcal{H}}^{(0)}(t_c) \} t_c \\ & + \int_0^{t_c} dt'_2 \int_0^{t'_2} dt'_1 \{ \bar{\mathcal{H}}^{(0)}(t_c) \bar{\mathcal{H}}(t'_2) \bar{\mathcal{H}}(t'_1) \} t_c] \\ & + P_{123} \bar{\mathcal{H}}^{(2)}(t_c). \end{aligned} \quad (\text{A13})$$

If $\bar{\mathcal{H}}^{(0)}(t_c)$ vanishes this leads, of course, immediately to

$$\bar{\mathcal{H}}^{(2)}(t_c) = P_{123} \bar{\mathcal{H}}^{(2)}(t_c), \quad (\text{A14})$$

with

$$\bar{\mathcal{H}}^{(2)}(t_c) = 0 \quad \text{if } P_{123} = -1.$$

Equation (A14) is also true if $\bar{\mathcal{H}}^{(0)}(t_c) \neq 0$, but P_{12}

$= P_{32} = +1$, since both integrals in Eq. (A13) vanish in this case, as shown in Appendix A1. Thus, it is shown that $\bar{\mathcal{H}}^{(2)}(t_c)$ vanishes for an antisymmetric cycle ($P_1 = P_2 = P_3 = -1$).

APPENDIX B

1. $\bar{\mathcal{H}}^{(1)}$ in LG Experiment

From Eq. (1b)

$$\bar{\mathcal{H}}^{(1)} = -i(2t_c)^{-1} \int_0^{t_c} dt_2 \int_0^{t_2} dt_1 [\bar{\mathcal{H}}(t_2), \bar{\mathcal{H}}(t_1)],$$

where $t_c = \tau_L$, we obtain

$$\begin{aligned} \bar{\mathcal{H}}^{(1)} = & -i(2t_c)^{-1} \int_0^{t_c} dt_2 \\ & \times \int_0^{t_2} dt_1 \{ [\bar{\mathcal{H}}_A(t_2), \bar{\mathcal{H}}_S(t_1)] + [\bar{\mathcal{H}}_S(t_2), \bar{\mathcal{H}}_A(t_1)] \}, \end{aligned} \quad (\text{B1})$$

since parts with $[\bar{\mathcal{H}}_S(t_2), \bar{\mathcal{H}}_S(t_1)]$ and $[\bar{\mathcal{H}}_A(t_2), \bar{\mathcal{H}}_A(t_1)]$ vanish for symmetry reasons.

Using Eqs. (42) and (43), Eq. (B1) yields

$$\begin{aligned} \bar{\mathcal{H}}^{(1)} = & -(2t_c)^{-1} \sum_{M_2 M_1} [\mathcal{H}(M_2), \mathcal{H}(M_1)] \int_0^{t_c} dt_2 \\ & \times \int_0^{t_2} dt_1 (\sin M_2 \omega_e t_2 \cos M_1 \omega_e t_1 \\ & + \cos M_2 \omega_e t_2 \sin M_1 \omega_e t_1), \end{aligned} \quad (\text{B2})$$

which leads to

$$\bar{\mathcal{H}}^{(1)} = \frac{t_c}{2\pi} \sum_{M \neq 0} \frac{1}{M} \{ 2[\mathcal{H}(M), \mathcal{H}(0)] + \frac{1}{2}[\mathcal{H}(-M), \mathcal{H}(M)] \}. \quad (\text{B3})$$

2. $\bar{\mathcal{H}}^{(2)}$ in LG Cycle

$\bar{\mathcal{H}}^{(2)}$ is, for symmetry reasons, the same in the LG cycle as in the FFLG cycle. Since the LG interaction Hamiltonian can be written as a sum of a symmetric and an antisymmetric part, we can apply the rules established in Sec. III, leaving us to evaluate only those integrals over the following commutator expressions over the LG cycle time τ_L :

$$\begin{aligned} & \{ \bar{\mathcal{H}}_S(t_3) \bar{\mathcal{H}}_A(t_2) \bar{\mathcal{H}}_A(t_1) \}, \\ & \{ \bar{\mathcal{H}}_A(t_3) \bar{\mathcal{H}}_A(t_2) \bar{\mathcal{H}}_S(t_1) \}, \\ & \{ \bar{\mathcal{H}}_A(t_3) \bar{\mathcal{H}}_S(t_2) \bar{\mathcal{H}}_A(t_1) \}. \end{aligned}$$

If we assume the average Hamiltonian to be zero, which is true for the dipolar Hamiltonian at the magic angle, we obtain

$$\bar{\mathcal{H}}_L^{(2)} = \frac{1}{6\tau_L} \sum_{M_3 M_2 M_1 \neq 0} \{ \mathcal{H}_D(M_3) \mathcal{H}_D(M_2) \mathcal{H}_D(M_1) \} X(\tau_L), \quad (\text{B4})$$

where

$$\begin{aligned}
X(\tau_L) &= \int_0^{\tau_L} dt_3 \int_0^{t_3} dt_2 \int_0^{t_2} dt_1 \\
&\times (\sin M_3 \omega_e t_3 \sin M_2 \omega_e t_2 \cos M_1 \omega_e t_1 \\
&+ \sin M_3 \omega_e t_3 \cos M_2 \omega_e t_2 \sin M_1 \omega_e t_1 \\
&+ \cos M_3 \omega_e t_3 \sin M_2 \omega_e t_2 \sin M_1 \omega_e t_1). \quad (\text{B5})
\end{aligned}$$

The following symmetry relations can be easily established:

$$\{\mathcal{F}(M_3) \mathcal{F}(M_2) \mathcal{F}(M_1)\} = \{\mathcal{F}(M_1) \mathcal{F}(M_2) \mathcal{F}(M_3)\} \quad (\text{B6})$$

and

$$\{\mathcal{F}(M_2) \mathcal{F}(M_2) \mathcal{F}(M_1)\} = -\frac{1}{2} \{\mathcal{F}(M_2) \mathcal{F}(M_1) \mathcal{F}(M_2)\}.$$

Using these relations and evaluating Eq. (B5), we

obtain

$$\bar{\mathcal{F}}_L^{(2)} = \frac{\tau_L^2}{6 \cdot 2^2 \pi^2} \sum_{M_3 M_2 M_1 \neq 0} \{\mathcal{F}(M_3) \mathcal{F}(M_2) \mathcal{F}(M_1)\} \times \Delta^F(M_3 M_2 M_1), \quad (\text{B7})$$

where $\Delta^F(M_3 M_2 M_1)$, given in Table I, obeys the following symmetry relations:

$$\Delta^F(M_3 M_2 M_1) = \Delta^F(M_1 M_2 M_3) \quad (\text{B8})$$

and

$$\Delta^F(M_3 M_2 M_1) = \Delta^F(-M_3 - M_2 - M_1).$$

3. $\bar{\mathcal{F}}^{(2)}$ in Six-Pulse Experiment

Using Eqs. (1), (42), (43), and (52), we obtain

$$\begin{aligned}
\bar{\mathcal{F}}_6^{(2)} &= -\frac{1}{6\tau_6} \sum_{M_3 M_2 M_1 \neq 0} \{\mathcal{F}(M_3) \mathcal{F}(M_2) \mathcal{F}(M_1)\} \left[\tau_w^3 \Delta^A(M_3 M_2 M_1) + \left(\frac{3}{2\pi}\right) \tau_w^2 \tau_p \Delta^B(M_3 M_2 M_1) \right. \\
&\quad \left. + \left(\frac{3}{2\pi}\right)^2 \tau_w \tau_p^2 \Delta^C(M_3 M_2 M_1) + \left(\frac{3}{2\pi}\right)^3 \tau_p^3 \pi \Delta^F(M_3 M_2 M_1) \right], \quad (\text{B9})
\end{aligned}$$

where $\Delta^F(M_3 M_2 M_1)$ is the same as for the FFLG and the LG experiment (Table I). All other Δ parameters obey the same symmetry relations [Eq. (B8)] as $\Delta^F(M_3 M_2 M_1)$. We obtain $\Delta^A(M_3 M_2 M_1)$ independent of M_2 and

$$\Delta^A(M_3 M_2 M_1) = \begin{cases} -\frac{1}{2} & \text{if } M_3 = M_1; \quad M_3 + M_1 = \pm 1 \text{ but } M_3 \neq M_1 \\ \frac{1}{4} & \text{otherwise.} \end{cases}$$

$\Delta^B(M_3 M_2 M_1)$ and $\Delta^C(M_3 M_2 M_1)$ are given in Table II.

APPENDIX C

1. $\bar{\mathcal{F}}^{(2)}$ for Nested-Cycle Type I

As in the six-pulse experiment,

$$\begin{aligned}
\bar{\mathcal{F}}_{SI}^{(2)} &= -\frac{2}{6t_c} \sum_{M_3 M_2 M_1 \neq 0} \{\mathcal{F}(M_3) \mathcal{F}(M_2) \mathcal{F}(M_1)\} \left[\tau_w^3 \Delta^A(M_3 M_2 M_1) + \frac{3}{(3n+1)2\pi} \tau_w^2 (n\tau_L + \tau_p) \Delta^B(M_3 M_2 M_1) \right. \\
&\quad \left. + \left(\frac{3}{(3n+1)2\pi}\right)^2 \tau_w (n\tau_L + \tau_p)^2 \Delta^C(M_3 M_2 M_1) + \left(\frac{3}{(3n+1)2\pi}\right)^3 (n\tau_L + \tau_p)^3 \pi \Delta^F(M_3 M_2 M_1) \right], \quad (\text{C1})
\end{aligned}$$

with $n\tau_L + \tau_p = (3n+1)\tau_p$ and $t_c = 2\tau_c$,

$$\bar{\mathcal{F}}_{SI}^{(2)} = -\frac{1}{6\tau_c} \sum_{M_3 M_2 M_1 \neq 0} \{\mathcal{F}(M_3) \mathcal{F}(M_2) \mathcal{F}(M_1)\}$$

TABLE I. Values of $\Delta^F(M_3 M_2 M_1)$ for Eq. (B7).

$M_3 \backslash M_1$	$M_2 = +1$				$M_3 \backslash M_1$	$M_2 = +2$			
	-2	-1	1	2		-2	-1	1	2
-2	0.0	$\frac{3}{4}$	$\frac{3}{4}$	0.0	-2	1.0	1.0	-1.0	$-\frac{1}{2}$
-1	$\frac{3}{4}$	4.0	-2.0	$-\frac{5}{4}$	-1	1.0	$-\frac{3}{2}$	$\frac{1}{2}$	0.0
1	$\frac{3}{4}$	-2.0	-0.0	$-\frac{1}{4}$	1	-1.0	$\frac{1}{2}$	$\frac{1}{2}$	0.0
2	0.0	$-\frac{5}{4}$	$-\frac{1}{4}$	0.0	2	$-\frac{1}{2}$	0.0	0.0	0.0

TABLE II. Values of (a): $\Delta^B(M_3M_2M_1)$, and (b): $\Delta^C(M_3M_2M_1)$ for Eq. (B9).

$M_3 \backslash M_1$		$M_2 = +1$				$M_3 \backslash M_1$		$M_2 = +2$			
		-2	-1	1	2			-2	-1	1	2
-2	-2	$-\sqrt{3}$	$\frac{3}{4}\sqrt{3}$	$\frac{1}{2}\sqrt{3}$	$\frac{1}{4}\sqrt{3}$	(a)	-2	$\frac{1}{2}\sqrt{3}$	$\frac{1}{2}\sqrt{3}$	$-\frac{3}{4}\sqrt{3}$	$-\frac{1}{4}\sqrt{3}$
-1	-1	$\frac{3}{4}\sqrt{3}$	$-3\sqrt{3}$	$\frac{1}{2}3\sqrt{3}$	$-\frac{7}{4}\sqrt{3}$	-1	$\frac{1}{2}\sqrt{3}$	$\sqrt{3}$	$\sqrt{3}$	$\frac{1}{2}\sqrt{3}$	$\frac{1}{2}\sqrt{3}$
1	1	$-\frac{1}{2}\sqrt{3}$	$\frac{3}{2}\sqrt{3}$	0.0	$\sqrt{3}$	1	$-\frac{3}{4}\sqrt{3}$	$\sqrt{3}$	$-2\sqrt{3}$	$\frac{1}{4}\sqrt{3}$	$\frac{1}{4}\sqrt{3}$
2	2	$\frac{1}{4}\sqrt{3}$	$-\frac{7}{4}\sqrt{3}$	$\sqrt{3}$	$-\frac{1}{2}\sqrt{3}$	2	$\frac{3}{4}\sqrt{3}$	$\frac{1}{2}\sqrt{3}$	$\frac{1}{4}\sqrt{3}$	0.0	0.0
(b)											
-2	-2	$\frac{9}{4}$	$-\frac{9}{8}$	$-\frac{9}{4}$	$-\frac{27}{16}$	-2	$-\frac{9}{4}$	$-\frac{27}{8}$	$\frac{27}{8}$	$\frac{45}{16}$	$\frac{45}{16}$
-1	-1	$-\frac{9}{8}$	-9.0	$\frac{45}{4}$	$\frac{9}{4}$	-1	$-\frac{27}{8}$	9.0	$\frac{9}{4}$	$-\frac{9}{8}$	$-\frac{9}{8}$
1	1	$-\frac{9}{4}$	$\frac{45}{4}$	0.0	$-\frac{9}{8}$	1	$\frac{27}{8}$	$\frac{9}{4}$	-9.0	$-\frac{27}{8}$	$-\frac{27}{8}$
2	2	$-\frac{27}{16}$	$\frac{9}{4}$	$-\frac{9}{8}$	0.0	2	$\frac{45}{16}$	$-\frac{9}{8}$	$-\frac{27}{8}$	0.0	0.0

$$\times \left[\tau_w^2 \Delta^A(M_3M_2M_1) + \frac{3}{2\pi} \tau_w^2 \tau_p \Delta^B(M_3M_2M_1) + \left(\frac{3}{2\pi}\right)^2 \tau_w \tau_p^2 \Delta^C(M_3M_2M_1) + \left(\frac{3}{2\pi}\right)^3 \tau_p^3 \pi \Delta^F(M_3M_2M_1) \right], \quad (C2)$$

which is the same expression as in the six-pulse experiment except for

$$\tau_c = 3(n\tau_L + \tau_w + \tau_p)$$

instead of $\tau_6 = 3(\tau_w + \tau_p)$. Thus

$$\overline{\mathcal{K}}_{SI}^{(2)} = \frac{\tau_6}{\tau_c} \overline{\mathcal{K}}_6^{(2)} = \frac{1}{1+m} \overline{\mathcal{K}}_6^{(2)}, \quad (C3)$$

where $m = n\tau_L / (\tau_w + \tau_p)$.

2. $\overline{\mathcal{K}}^{(2)}$ for Nested Cycles of Type II

We find

$$\overline{\mathcal{K}}_{SI}^{(2)}(t_c) = (1/t_c)(2n\tau_L \overline{\mathcal{K}}_L^{(2)} + 2\tau_p \overline{\mathcal{K}}_p^{(2)}), \quad (C4)$$

where $t_c = 2n\tau_L + 2\tau_p$. If

$$\overline{\mathcal{K}}_L^{(2)} = -\tau_L^2 A \quad (C5)$$

and

$$\overline{\mathcal{K}}_p^{(2)} = -\tau_p^2 B,$$

we obtain

$$\overline{\mathcal{K}}_{SI}^{(2)} = -(n\tau_L^2 A + \tau_p^2 B) / (n\tau_L + \tau_p). \quad (C6)$$

In order to make an estimate, we assume for simplicity $A = B$, i. e., $\overline{\mathcal{K}}_L^{(2)} = \overline{\mathcal{K}}_p^{(2)}$ for $\tau_L = \tau_p$. We obtain

$$\overline{\mathcal{K}}_{SI}^{(2)} = [(n+M^3)/(nM^2+M^3)] \overline{\mathcal{K}}_6^{(2)}, \quad (C7)$$

where $M = \tau_p / \tau_L = 1 + 3\tau_w / \tau_L$.

*Work supported in part by the National Science Foundation.

†Present address: Physikalisches Institut der Universität Münster, 44 Münster, Germany.

¹A. Abragam, *The Principles of Nuclear Magnetism* (Oxford U. P., Oxford, 1961), p. 103.

²A. G. Redfield, *Phys. Rev.* **98**, 1787 (1955).

³U. Haeberlen and J. S. Waugh, *Phys. Rev.* **185**, 420 (1969).

⁴A. R. Edmonds, *Angular Momentum in Quantum Mechanics* (Princeton U. P., Princeton 1960), p. 72.

⁵E. R. Andrew, A. Bradbury, and R. G. Eades, *Arch. Sci. (Geneva)* **11**, 223 (1958).

⁶I. J. Lowe, *Phys. Rev. Letters* **2**, 285 (1959).

⁷M. Lee and W. I. Goldberg, *Phys. Rev.* **140**, A1261 (1965).

⁸E. D. Ostroff and J. S. Waugh, *Phys. Rev. Letters* **16**, 1097 (1966).

⁹J. S. Waugh, L. M. Huber, and U. Haeberlen, *Phys. Rev. Letters* **20**, 180 (1968).

¹⁰U. Haeberlen and J. S. Waugh, *Phys. Rev.* **175**, 453

(1968).

¹¹M. Mehring, R. G. Griffin, and J. S. Waugh, *J. Am. Chem. Soc.* **92**, 7222 (1970).

¹²L. M. Stacey, R. W. Vaughan, and D. D. Elleman, *Phys. Rev. Letters* **26**, 1153 (1971).

¹³M. Mehring, R. G. Griffin, and J. S. Waugh, *J. Chem. Phys.* **55**, 746 (1971).

¹⁴W. K. Rhim, A. Pines, and J. S. Waugh, *Phys. Rev. B* **3**, 684 (1971).

¹⁵P. Mansfield, *J. Phys. C* (to be published).

¹⁶A. Pines, W. K. Rhim, and J. S. Waugh, presented at the Fourth International Symposium on Magnetic Resonance, Rehovot and Jerusalem, Israel, 1971 (unpublished); *J. Mag. Res.* (to be published).

¹⁷J. D. Ellett, Ph. D. thesis (MIT, 1970) (unpublished).

¹⁸F. Bloch and A. Siegert, *Phys. Rev.* **57**, 522 (1940).

¹⁹J. D. Ellett *et al.*, *Advanced Magnetic Research*, (Academic, New York, 1971), Vol. 5.

²⁰J. D. Ellett, U. Haeberlen, and J. S. Waugh, *Polymer Letters* **7**, 71 (1969).

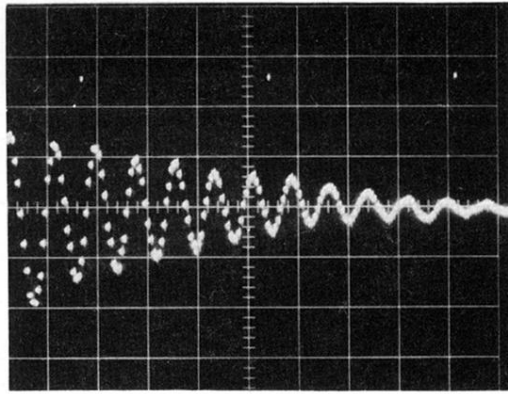


FIG. 4. Decay of F^{19} in CaF_2 as observed in a nest-cycle type-I experiment. Horizontal: $50 \mu\text{sec}/\text{point}$, window width $\tau_w = 4.5 \mu\text{sec}$, cycle time $t_c = 85 \mu\text{sec}$. The decay time is approximately 5 msec , corresponding to a linewidth of 68 Hz .